Advances in Science and Technology Research Journal

Advances in Science and Technology Research Journal 2024, 18(2), 365–373
https://doi.org/10.12913/22998624/185270
ISSN 2299-8624, License CC-BY 4.0

Received: 2024.02.05
Accepted: 2024.02.23
Published: 2024.03.15

Time-Resolved Sensitivity of a Cadmium-Doped Copper Oxide Thin Film as a Chlorine Gas Detector

Turki Alotibi[1], Waleed Shirbeeny[1*], Ahmed Alshahrie[1], Mohammed Aida[1], Jawid Iqbal[2]

[1] Department of Physics, King Abdulaziz University, Jeddah, Saudi Arabia
[2] Center of Nanotechnology, King Abdulaziz University, Jeddah, Saudi Arabia
* Corresponding author's e-mail: wshirbeeny@kau.edu.sa

ABSTRACT

Due to its strong affinity for chlorine gas, Cd can potentially form $CdCl_2$. Cd-doped CuO thin films are sensitive to chlorine gas, as careful inclusion of Cd in the CuO crystal structure modifies the energy gap depending on the dopant concentration. We employed spray pyrolysis to deposit Cd-doped CuO on fluorine tin oxide (FTO) while heating the substrate to 500 °C. The X-ray diffraction (XRD) analysis revealed that Cd was interstitially incorporated in the CuO lattice structure, as verified by scanning electron microscopy (SEM) imaging. The photoluminescence study demonstrated that increasing the Cd concentration in CuO resulted in higher emission intensity, providing valuable insights into Cu^{2+} and O^{2-} energy levels. Exposing a Cd-doped CuO thin film to chlorine gas modifies the bandgap, depending on the Cd concentration. The fluctuation in the bandgap energy of copper oxide doped with cadmium indicates the chlorine gas concentration nearby. Time-resolved measurements for the I-V characteristics of the thin film revealed considerable current variation during the exposure to chlorine gas.

Keywords: sensor, bandgap, affinity, spray pyrolysis, time-resolved.

INTRODUCTION

Metal oxides have recently emerged as a captivating area of interest in materials research [1, 2]. One such oxide is copper oxide (CuO), a p-type semiconductor boasting an optical band gap (Eg) ranging from approximately 1.2 to 1.9 eV. CuO has garnered considerable attention due to its distinct properties, positioning it as a potential candidate for diverse applications like gas sensors [3, 4, 5], optoelectronic devices [6, 7, 8], solar cells [9, 10, 11], supercapacitors [12, 13] and cells [14, 15]. Previous studies have explored the enhancement of CuO chemical properties by investigating the impact of doping transition metals such as Li [16], Ni [17], Zn [18], Mn [19], and Cd [20], among others. However, limited research has been conducted on Cd-doped CuO. Various deposition techniques have been employed by some researchers, including the hydrothermal method [20, 21]. Additionally, alternative approaches such as the gel method [22], simple chemical precipitation method [23], and spray pyrolysis technique [24] have also been utilized. Among these methods, the spray pyrolysis technique is cost-effective and straightforward since it does not necessitate high-quality substrates. Moreover, this approach provides benefits, like regulation of film placement and the capability to apply films across regions [25, 26].

The main objective of this research is to improve the optoelectronic properties of Cd-doped CuO specifically for gas sensing applications. The focus is on incorporating Cd into the crystal structure of CuO in a controlled manner to decrease the energy gap of the thin films, thereby improving their sensing capabilities. The deposition of Cd-doped CuO onto FTO substrates was achieved using the spray pyrolysis technique while heating the substrate to 500 °C to facilitate the introduction of Cd into the interstitial sites. This intentional adjustment in the composition

would enable the future detection of chlorine gas. Cd's strong affinity for Cl and its deliberate incorporation selectively disrupt specific bonds in CuO, allowing for the preferential combination of Cd^{2+} with any expected Cl^{2-}.

METHODOLOGY

Chemicals and materials

Copper acetate monohydrate (99% purity) [$Cu(CH_3COO)_2.H_2O$] and cadmium chloride (laboratory reagent) [$CdCl_2.H_2O$] were employed as the copper and cadmium precursors, respectively. These substances were utilized in their original form without further treatment or modifications.

Samples preparation and materials synthesis

Cd-doped CuO thin films were fabricated using the spray pyrolysis technique on FTO-on-glass substrates. Before drying with nitrogen (N_2) gas, the FTO glass substrates underwent a cleaning process involving methanol, ethanol, and acetone, then rinsing with deionized (DI) water. The reaction procedure involved dissolving 0.1 M of $Cu(CH_3COO)_2.H_2O$ and $CdCl_2.H_2O$ into 40 ml of DI water at room temperature (RT). The solutions were stirred until a homogeneous mixture was achieved. Subsequently, three different Cd concentrations (0.1%, 0.2%, and 0.4%) were prepared. During the deposition process, the distance between the substrate surface and the spray nozzle was adjusted and maintained at approximately 15 cm. The deposition operation involved the controlled flow of the solution from the spray nozzle at a constant rate of around 0.84 ml/min. At the same time, the temperature of the substrate was maintained at 500 °C. After deposition, the fabricated films were allowed for 2 hours to cool down to RT. The specific parameters and conditions employed for preparing Cd-doped CuO thin films are summarized in Table 1.

Gas detection and activation temperature

When investigating the behavior of a film doped with Cd on an FTO substrate as a sensor for chlorine gas, we can observe changes in the sensing response over time and at different activation temperatures [22].

Table 1. Deposition parameters of Cd-doped CuO thin films

Parameter	Condition
Substrate temperature	500 °C
Nozzle-substrate distance	15 cm
Solution flow rate	0.84 ml/min
Solution volume	40 ml
deposition time	8 min

Activation energy – by adjusting the temperature, we can notice variations in the activation energy of the sensing process. The current flowing through the film may demonstrate temperature tendencies, such as increasing or decreasing with rising temperatures. Determining the activation energy allows us to understand how the sensing mechanism works.

Time response – upon exposure to chlorine gas, the current passing through the film may exhibit time-related patterns. Initially, current changes might indicate a response to the gas. However, over time, factors like diffusion, surface reactions, or alterations in the properties of the film could cause stabilization or gradual changes in the current.

Chlorine gas can interact with the interstitially doped Cd in CuO thin film and change the thin film's electrical properties. However, this interaction depends on the activation temperature of the sensor. A ceramic electric heating plate has provided the temperature source with a maximum temperature of 90 °C.

CHARACTERIZATION TECHNIQUES

The crystal structure of Cd-doped CuO thin films was characterized using X-ray diffraction (XRD) analysis. The XRD measurements were performed on an Ultima IV instrument (Rigaku, Japan) equipped with Cu-Kα radiation (wavelength = 1.54060 Å) and operated at a voltage of 40 kV. The obtained XRD data was processed using MATCH! Software from Crystal Impact. A UV-visible-near-infrared (UV-vis-NIR) spectrophotometer (Lambda 750, PerkinElmer) was employed to inspect the optical properties of the films. The photoluminescence emission spectrum was obtained at room temperature using a Spectro fluorophotometer (RF-5301pc, Shimadzu). A field emission scanning electron microscope (Quanta 250, FEI,

FP 2012/14) examined the surface morphology of the prepared films. Two Leybold Didactic GMBH sensor-CASSY were used for current I versus time t and temperature T measurements. A constant DC voltage of 1.1 V was maintained during the gas detection with a base current of 0.759 A. The sensor activation temperature was provided using a ceramic electric heating plate operated by 220 V AC power.

RESULTS AND DISCUSSION

XRD investigation

The study of Cd-doped CuO at Cd concentrations 0.1%, 0.2%, and 4% revealed the XRD pattern displayed in Figure 1, with the FTO diffraction pattern subtracted. According to the Crystallography Open Database card COD # [96-410-5686], the Cd-doped CuO unit cell is monoclinic. No phase change occurred with the addition of more Cd concentrations. However, the CuO diffraction lines (110), (002), (111), and (021), which appeared at the diffraction angles (2θ = 33.25, 35.76, 38.59, and 55.61°), had their positions slightly red-shifted due to the interstitial corporation of more Cd into the CuO crystal. Additionally, the diffraction intensities decreased by increasing Cd concentration. The decrease in intensity of the CuO diffraction lines can be attributed to the Cd diffraction centers' dominance over CuO [28, 29]. The basic Scherrer equation [27] (1) estimated the crystallite size G. Where k is Scherrer constant and is taken at 0.9, FWHM is the full width at half maximum of the most intense peak. The d-spacing and the grain (crystallite) size were influenced by the increase in Cd concentration and are listed in Table 2. A decrease in the d-spacing was observed as the Cd concentration increased. This reduction in interplanar spacing is attributed to incorporating Cd between the atomic planes, resulting in strain within the crystalline structure. However, it should be noted that the grain size exhibited a slight decrease as the Cd concentration increased. There could be a few reasons for the slight reduction in grain size with higher Cd concentration in Cd-doped CuO thin films. In "Crystal Growth Inhibition" [30], Cd atoms in the CuO lattice may inhibit the crystal growth, leading to smaller grain sizes. In addition, Cd impurities may alter the surface energy [31, 32] of the growing film, affecting the grain boundaries and resulting in smaller grain sizes. Higher Cd concentrations may also intensify film stress and strain, impeding grain growth and leading to smaller grain sizes.

$$G = \frac{k\,\lambda}{FWHM\cos\theta} \tag{1}$$

where: G is the grain size, FWHM is the full width at half maximum of the selected maximum at the specified Muller indices (hkl), k is the shape factor taken 0.9, 2θ is the diffraction angle as a function of (hkl), and λ is the X-ray wavelength (1.5406 Å).

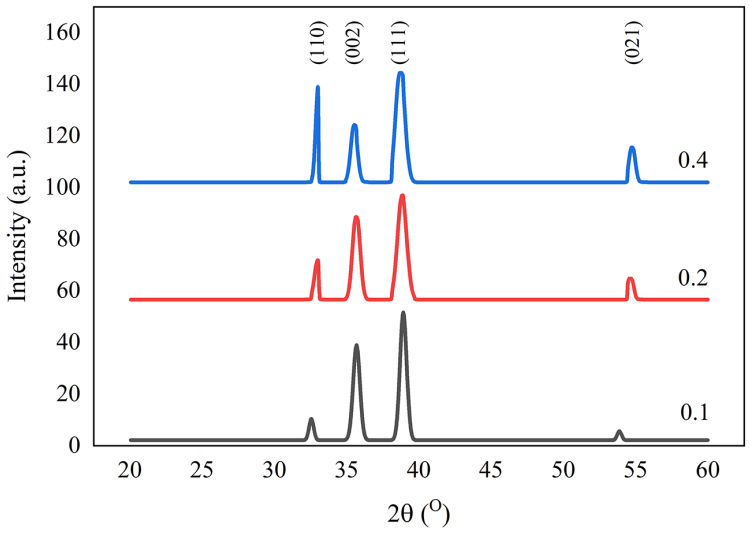

Figure 1. The X-ray diffraction (XRD) pattern of thin films of CuO doped with different concentrations of Cd (0.1%, 0.2%, and 0.4%) was measured at room temperature

Table 2. The Cd-doped CuO lattice parameters

Conc.	2θ	*hkl*	FWHM ± σ x 10^{-4}	G	*d*	*a*	*b*	*c*	*β*
	deg		Rad.	Å					deg
0.1%	32.55	110	0.00734 ± 1.4	196.6	2.748	4.289	3.613	5.095	80.7
0.2%	33.16		0.00734 ± 1.4	196.6	2.699	4.252	3.504	2.055	84.2
0.4%	33.25		0.00834 ± 1.7	173.2	2.692	4.227	3.497	5.029	85.9

SEM and surface morphology characterization

The examination of surface morphology revealed that the Cd ions did not replace the Cu ions within the structure of CuO. Instead, they occupied interstitial positions, evidenced by surface characterization of the thin film. Cd manifested as bright grains on the surface, in contrast to CuO. Furthermore, the investigation of surface properties indicated that the average particle size for CuO: Cd 0.0.1% was approximately 155 nm ± 15. For Cd 0.2%, the average particle size increased to around 275 nm ± 18, while for CuO: Cd 0.4%, the average particle size was approximately 376 nm ± 20. The top surface views of the thin film for each of these sizes can be observed in Figure 2A, 2B, and 2C, while an inclined view at a 50° angle to the surface is depicted in Figure 2D, 2E, and 2F. Overall, the thin film surface displayed high uniformity and homogeneity.

Elemental verification

By employing an energy-dispersive X-ray (EDX) technique, we could analyze a specific film region and determine the elemental composition of Cd-doped CuO. The EDX investigation showed an absorption edge at 3.134 keV, corresponding to the L_α transition. The elemental composition analysis confirmed that the Cd-doped CuO consisted solely of the targeted elements. The elements ratios were 30.02, 65, and 4.98 wt% for oxygen, copper, and cadmium, respectively.

Optical characterization

Transmittance spectroscopy was conducted on thin films of Cd-doped CuO to investigate their optical characteristics at the underlying Cd concentrations. Figure 3A illustrates notable variations in transmittance among the three films. It is

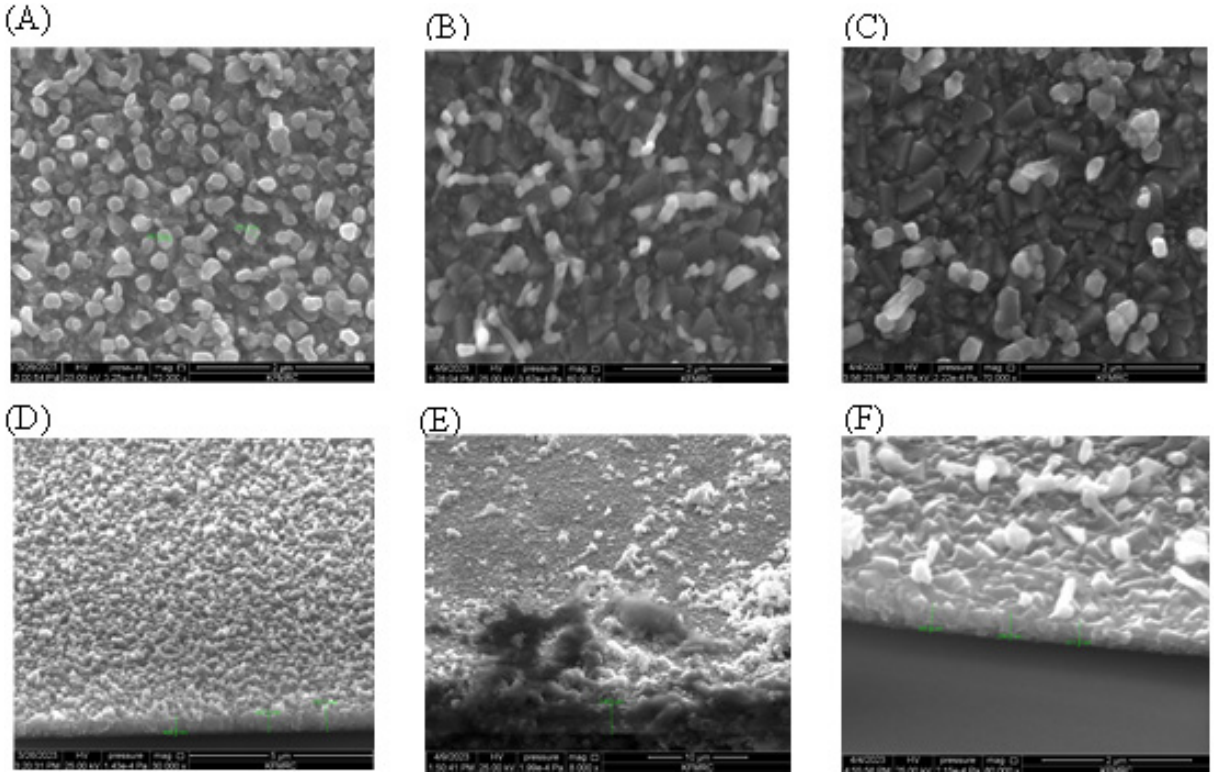

Figure 2. Top view (A), (B), and (C) and 50°-inclined view (D), (E), and (F) of the three Cd concentrations, 0.1. 0.2, and 0.4, respectively, taken at room temperature

noticeable that the transmission increased as the Cd concentration increased. Figure 3B presents the Tauc plot and provides valuable insights into the semiconductor's band gap characteristics. According to Tauc's equation:

$$(\alpha h\nu)^n = K(h\nu - E_g) \quad (2)$$

where: K is an energy-independent constant, a is the absorption coefficient, h is the Planck constant, Eg is the bandgap energy, and n indicates the direct or indirect bandgap energy. n=1/2 for allowed indirect bandgap and is 2 for allowed direct bandgap

It revealed that the Cd-doped CuO thin films exhibited direct band gaps, with values of 1.61 eV, 1.45 eV, and 1.29 eV for Cd concentrations of 0.1%, 0.2%, and 0.4%, as seen in the Figure 3B.

Interestingly, although Cd does not replace the Cu ions within the CuO crystal structure, the Cd introduction reduced the thin film's band gap energy. The material's electronic structure is modified by introducing Cd atoms, which have electronic properties different from Cu, into the CuO crystal lattice. The Cd impurities introduced new energy levels within the band structure. These new energy levels created by Cd atoms can lower the conduction band's energy, raise the valence band's energy, or both [33]. As a result, the band gap energy of the Cd-doped CuO thin film is reduced compared to the pure CuO material.

Photoluminescence characterization

The investigation of photoluminescence in Cd-doped CuO thin films demonstrated that the presence of Cd in CuO crystal lattice with increasing concentration enhanced the emission intensity of the film. This increase in emission intensity can be observed in Figure 4A. The emission intensity enhancement by adding more Cd to the CuO structure can be ascribed to defect-related emission centers [34]. Cd impurities can introduce defect states or vacancy sites within the CuO crystal lattice. These defect sites can serve as emission centers, promoting radiative transitions and contributing to the enhanced emission intensity observed in the film. In a careful study of the deconvoluted photoluminescence spectra for the Cd concentration of 0.1%, a single emission line belonging to Cu^{2+} was observed at approximately 382.60 ± 2.0 nm. This emission corresponds to the transition $^0[213311]_{7/2} \rightarrow {}^1[239440]_{7/2}$ [35]. Also, an emission line of O^{2-} was observed at approximately 431.78 ± 3.5 nm, corresponding to an energy level of 2.87 eV in the conduction band. Adding more Cd concentration to the structure changed the emission line's position for oxygen ions. In addition, two Cu^{2+} emission lines were observed at 381.35 ± 0.1 nm and 392.35 ± 0.1 nm for a Cd concentration of 0.2%. For a Cd concentration of 0.4%, the Cu^{2+} emission lines were observed at 381.6 ± 1.0 nm and 393.85 ± 1.6 nm. The shifts in Cu and O emission lines are attributed to the increase in Cd concentration. The emission lines [36] and their variations are listed in Table 3. The emission lines due to Cu^{2+} and O^{2-} are depicted in Figure 4B, 4C, and 4D. The emission centers of Cu^{2+} and O^{2-} are responsible for the emission enhancement in Figure 4A.

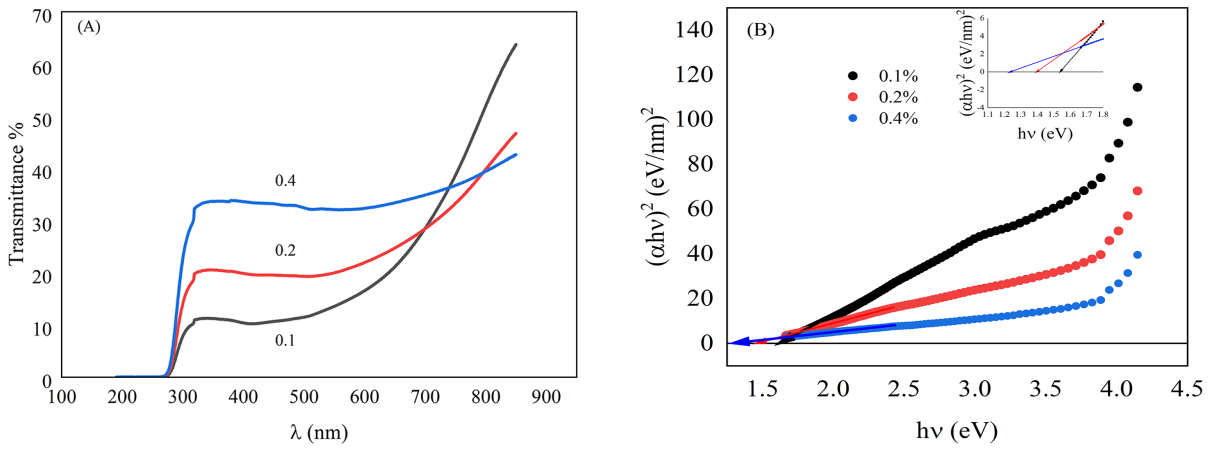

Figure 3. (A) The transmittance spectrum of the underlying Cd concentrations, measured at roome temperaturej, (B) Tauc plot for the Cd-doped CuO thin films

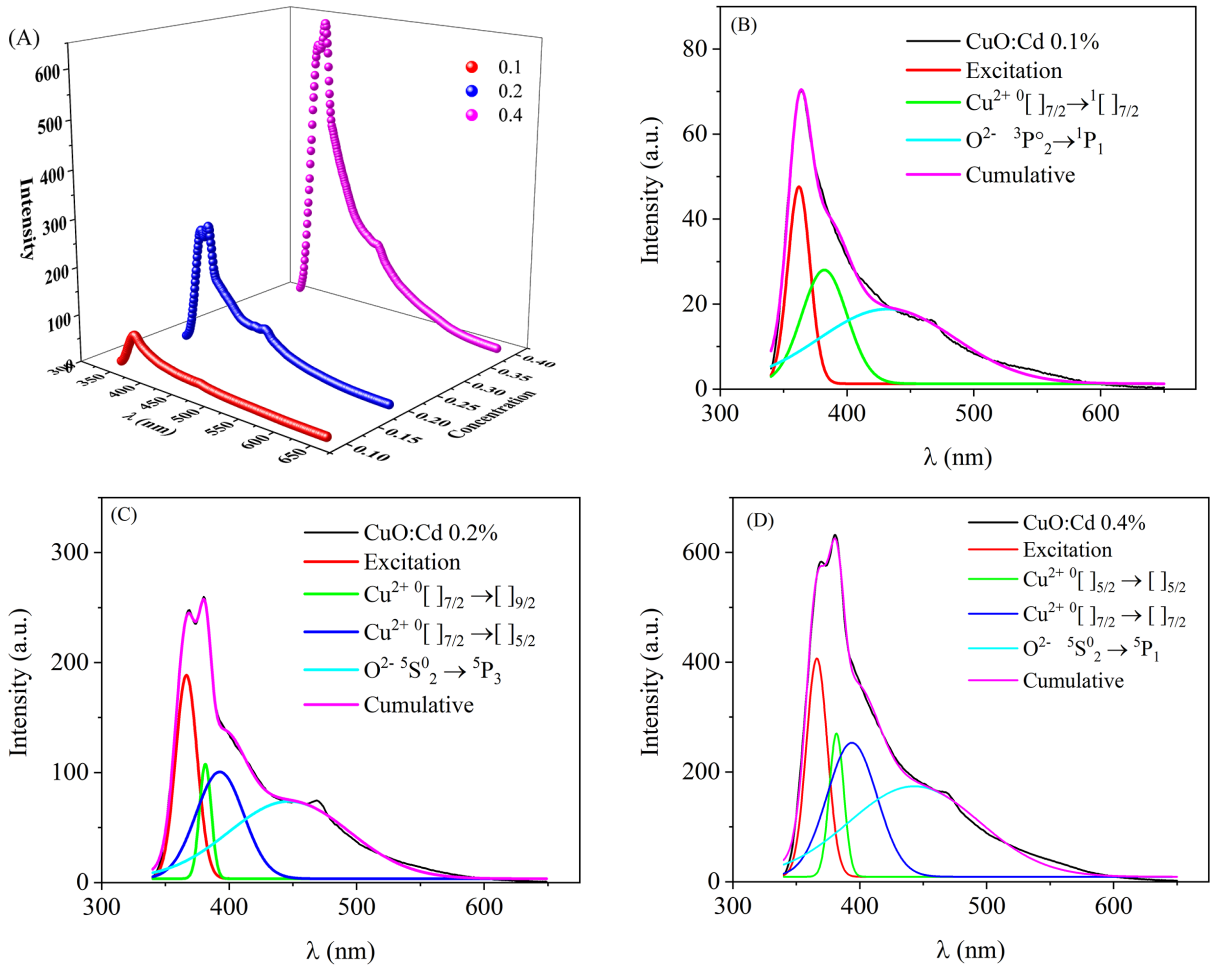

Figure 4. The PL spectra, measured at room temperature, of the Cd-doped CuO thin films

Table 3. The emission lines, obtained at room temperature, of the Cu^{2+} and O^{2-}

Cd conc.		Line (nm)	Transition (cm^{-1})	
0.1%	Cu^{2+}	382.60±2.0	$^{0}[213311]_{7/2}$	$[239440]_{7/2}$
	O^{2-}	431.78±3.5	$^{3}P^{0}_{2}$	$^{1}P_{1}$
0.2%	Cu^{2+}	381.35±0.1	$^{0}[215000]_{7/2}$	$[241215]_{9/2}$
		392.35±1.0	$^{0}[232435]_{7/2}$	$[257885]_{5/2}$
	O^{2-}	447.15±1.9	$^{5}S^{0}_{2}$	$^{5}P_{3}$
0.4%	Cu^{2+}	381.69±0.2	$^{0}[228423]_{5/2}$	$[254620]_{5/2}$
		393.85±1.6	$^{0}[213311]_{7/2}$	$[238638]_{7/2}$
	O^{2-}	443.03±3.0	$^{5}S^{0}_{2}$	$^{5}P_{1}$

Gas detection by Cd-doped CuO thin film

The heating plate has been attached to the glass side of the FTO-on-glass substrate using thermal paste, as seen in Figure 5A and 5B are contact probes. A constant DC voltage of 1.1 Volts was applied to the thin film, and a minimum current of 0.759 A passed through the thin film simultaneously. Two CASSYLAB modules were used to supply the biasing voltage and to record the current with time, and the 2nd module was used for measuring temperature with time. The composition was put into an electrochemical cell with a cap providing a closed circumference with an inlet switch for the gas supply.

Starting with an activator temperature of 27°C and at a running time of about 50 s, the activator power supply was started simultaneously with the running time. The system recorded the current against running time, and a thermocouple

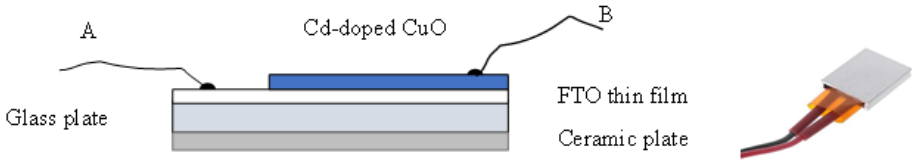

Figure 5. Schematic of the Cd-doped CuO thin film deposited on FTO with ceramic heating plate attached

recorded the accompanying activator temperature. We allowed the gas to flow constantly during a specific time interval and cut it off. We repeated the on-off gas allowance routine three times, deonted in the Figure 6 by thee-ONs, until the activator temperature reached its maximum value, and then we stopped the run. The time-temperature-gas flow current dependence was recorded and displayed in Figure 6. In addition, the current intensity exhibited an activation temperature dependence. The sensor's responsivity to the gas flow increased as the activation temperature increased. The response time can be approximately 5.4 seconds, and the recovery time can be 10 seconds.

It can be inferred that the Cd concentration of 0.4 in the CuO matrix is the most effective in detecting or responding to the specific gas being tested, the maximum response was about 0.002 A. This finding suggests that the higher concentration of Cd in the CuO material enhances its gas-sensing properties, potentially due to increased surface area or improved interaction with the gas molecules. Other lower Cd concentrations did not give a response to the gas, so they were not included in the results.

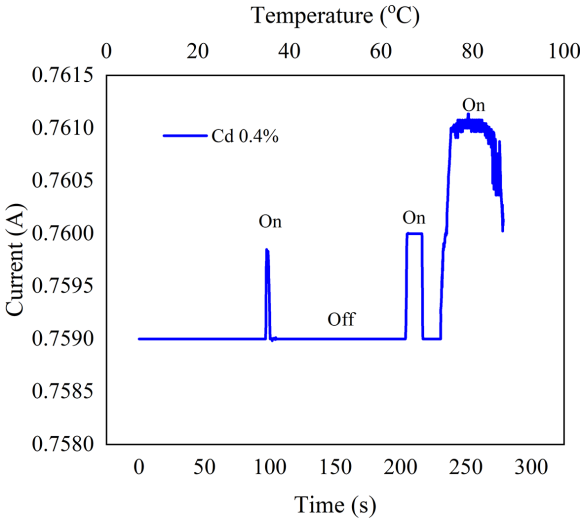

Figure 6. The current dependence on the gas flow and activation temperature for the Cd-doped at Cd concentration 0.4%

CONCLUSIONS

The deposition of Cd-doped CuO on an FTO-on-glass substrate was successfully achieved using the spray pyrolysis deposition method at a temperature of 500 °C. X-ray diffractio analysis confirmed that Cd did not replace Cu in the CuO structure but occupied interstitial sites within the lattice. The scanning electron microscopy technique was employed to investigate and analyze the surface morphology and thickness of the Cd-doped CuO films, revealing uniform thickness and a homogeneous composition across the films.

UV-visible spectroscopy was employed to investigate the absorption properties of the Cd-doped CuO films with varying concentrations of Cd. It was observed that the absorption decreased as more Cd was added to the CuO, indicating changes in the material's light absorption characteristics. Additionally, the band gap energies of the Cd-doped CuO films decreased as the Cd concentration increased.

Photoluminescence investigations were conducted, and it was found that the emission intensity increased with higher Cd concentrations in the CuO films. The positions of the emission lines associated with Cu^{2+} ions were not preserved upon adding Cd to the thin films.

These findings suggest the potential use of Cd-doped CuO films as gas sensors, particularly for detecting chlorine gas. Cd exhibits a strong affinity for chlorine gas, resulting in variations in the energy gap of the material. These variations can be seen by an external I-V circuit, highlighting the potential of Cd-doped CuO films for gas sensing applications.

The lower concentrations of Cd showed no response to the gas passage. However, the 0.4 Cd concentration revealed a noticeable influence on the Current passing through the thin film, indicating the suitable dopant concentration for this sensor to be affected by the chlorine gas.

REFERENCES

1. T. Jiang, J. Kong, Y. Wang, D. Meng, D. Wang, and M. Yu, Optical and Photocatalytic properties of Mn-doped CuO nanosheets prepared by hydrothermal method. Cryst. Res. Technol., 51(1), 58–64, 2016, doi: 10.1002/crat.201500152.
2. S.D. Al Ghamdi, A. O. M. Alzahrani, M. S. Aida, and M. S. Abdel-wahab, Influence of substrate temperature and solution molarity on CuO thin films' properties prepared by spray pyrolysis. J. Mater. Sci. Mater. Electron., 33(18), 14702–14710, Jun. 2022, doi: 10.1007/s10854-022-08390-8.
3. H. Bai et al., Light-activated ultrasensitive NO2 gas sensor based on heterojunctions of CuO nanospheres/MoS2 nanosheets at room temperature. Sensors Actuators B Chem., 368, 132131, 2022, doi: https://doi.org/10.1016/j.snb.2022.132131.
4. N. Wang et al., Highly sensitive and selective NO2 gas sensor fabricated from Cu2O-CuO microflowers. Sensors Actuators B Chem., 362, 131803, 2022, doi: https://doi.org/10.1016/j.snb.2022.131803.
5. A. Kumar, A. K. Shringi, and M. Kumar, RF sputtered CuO anchored SnO2 for H2S gas sensor. Sensors Actuators B Chem., 370, 132417, 2022, doi: https://doi.org/10.1016/j.snb.2022.132417.
6. Z. Yin et al., Multifunctional optoelectronic device based on CuO/ZnO heterojunction structure. J. Lumin., 257, 119762, 2023, doi: https://doi.org/10.1016/j.jlumin.2023.119762.
7. M.A. Khan et al., Interface study of hybrid CuO nanoparticles embedded ZnO nanowires heterojunction synthesized by controlled vapor deposition approach for optoelectronic devices. Opt. Mater. (Amst)., 117, 111132, 2021, doi: https://doi.org/10.1016/j.optmat.2021.111132.
8. G. Sreedevi, K. Srinivas, M. Subbarao, and S. Cole, Investigation on structural and optical properties of CuO doped CdS-$Zn_3(PO_4)_2$ nanocomposite for optoelectronic devices. J. Mol. Struct., 1222, 128903, 2020, doi: https://doi.org/10.1016/j.molstruc.2020.128903.
9. D. Naveena, R. Dhanabal, and A. Chandra Bose, Investigating the effect of La doped CuO thin film as absorber material for solar cell application. Opt. Mater. (Amst)., 127, 112266, 2022, doi: https://doi.org/10.1016/j.optmat.2022.112266.
10. V.T. Babu et al., Role of front and back contacts in the performance of TiO_2/CuO heterojunction solar cells. Mater. Today Proc., 65, 408–415, 2022, doi: https://doi.org/10.1016/j.matpr.2022.07.199.
11. W. Shirbeeny and F. Talbi, Improved photon trapping by combined use of dye-synthesized and one-dimensional fiber-like nanostructured CuO thin film. Optik (Stuttg), 147, 14–21, 2017, doi: 10.1016/j.ijleo.2017.08.076.
12. N. Indumathi, C. Sridevi, A. Gowdhaman, and R. Ramesh, Synthesis, structural analysis, and electrochemical performance of chitosan incorporated CuO nanomaterial for supercapacitor applications. Inorg. Chem. Commun., 156, 11222, 2023, doi: https://doi.org/10.1016/j.inoche.2023.111222.
13. J. Zhang, R. Huang, Z. Dong, H. Lin, and S. Han, An illumination-assisted supercapacitor of rice-like CuO nanosheet coated flexible carbon fiber. Electrochim. Acta, 430, 140789, 2022, doi: https://doi.org/10.1016/j.electacta.2022.140789.
14. F.Z. Chafi, L. Bahmad, N. Hassanain, B. Fares, L. Laanab, And A. Mzerd, Characterization techniques of fe-doped cuo thin films deposited by the spray pyrolysis method. arXiv, July, 2018.
15. M.H. Kabir, H. Ibrahim, S. A. Ayon, M. M. Billah, and S. Neaz, Structural, nonlinear optical and antimicrobial properties of sol-gel derived, Fe-doped CuO thin films. Heliyon, 8(9), e10609, 2022, doi: 10.1016/j.heliyon.2022.e10609.
16. I. . Zgair, A. H. Omran Alkhayatt, A. A. Muhmood, and S. K. Hussain, Investigation of structure, optical and photoluminescence characteristics of Li doped CuO nanostructure thin films synthesized by SILAR method. Optik (Stuttg)., 191, June, 48–54, 2019, doi: 10.1016/j.ijleo.2019.06.008.
17. S. Baturay et al., Modification of electrical and optical properties of CuO thin films by Ni doping. J. Sol-Gel Sci. Technol., 78(2), 422–429, 2016, doi: 10.1007/s10971-015-3953-4.
18. M. Nesa, M. Sharmin, K. S. Hossain, and A. H. Bhuiyan, Structural, morphological, optical and electrical properties of spray deposited zinc doped copper oxide thin films. J. Mater. Sci. Mater. Electron., vol. 28, no. 17, pp. 12523–12534, 2017, doi: 10.1007/s10854-017-7075-3.
19. R. Rahaman, M. Sharmin, and J. Podder, Band gap tuning and p to n-type transition in Mn-doped CuO nanostructured thin films. J. Semicond., 43(1), 2022, doi: 10.1088/1674-4926/43/1/012801.
20. Y. Wang, T. Jiang, D. Meng, D. Wang, and M. Yu, "Synthesis and enhanced photocatalytic property of feather-like Cd-doped CuO nanostructures by hydrothermal method," Appl. Surf. Sci., 355, 191–196, Nov. 2015, doi: 10.1016/j.apsusc.2015.07.122.
21. D. Wang, Y. Wang, T. Jiang, H. Jia, and M. Yu, The preparation of M (M: Mn^{2+}, Cd^{2+}, Zn^{2+})-doped CuO nanostructures via the hydrothermal method and their properties. J. Mater. Sci. Mater. Electron., 27(2), 2138–2145, Feb. 2016, doi: 10.1007/s10854-015-4003-2.
22. D. Sivayogam, I. Kartharinal Punithavathi, S. Johnson Jayakumar, and N. Mahendran, Structural, optical and electrical properties of Cd doped CuO nanoparticles obtained by simple sol gel method. Mater. Today Proc., 49, 2752–2757, 2021, doi:

10.1016/j.matpr.2021.09.291.

23. S. Ramya, R. Gobi, N. Shanmugam, G. Viruthagiri, and N. Kannadasan, Investigation on the structural, optical, morphological and magnetic properties of undoped and Cd doped CuO nanoflakes. J. Mater. Sci. Mater. Electron., 27(1), 40–48, 2016, doi: 10.1007/s10854-015-3714-8.
24. M.H. Babu, J. Podder, B. C. Dev, and M. Sharmin, P to n-type transition with wide blue shift optical band gap of spray synthesized Cd doped CuO thin films for optoelectronic device applications. Surfaces and Interfaces, 19, 100459, 2020, doi: 10.1016/j.surfin.2020.100459.
25. S. Kose, E. Ketenci, V. Bilgin, F. Atay, and I. Akyuz, Some physical properties of in doped copper oxide films produced by ultrasonic spray pyrolysi. Curr. Appl. Phys., 12(3), 890–895, 2012, doi: 10.1016/j.cap.2011.12.004.
26. S.K. Shinde et al., Effect of deposition parameters on spray pyrolysis synthesized CuO nanoparticle thin films for higher supercapacitor performance. J. Electroanal. Chem., 850, 113433, 2019, doi: 10.1016/j.jelechem.2019.113433.
27. V. Krasinskyi, L. Dulebova, I. Gajdos, O. Krasinska, and T. Jachowicz, Study of crystalline and thermal properties of nanocomposites based on polyamide-6 and modified montmorillonite. Adv. Sci. Technol. Res. J., 17(6), 88–97, Dec. 2023, doi: 10.12913/22998624/174180.
28. M. Sarwar et al., Crystal lattice damage and recovery of rare-earth implanted wide bandgap oxides. Adv. Sci. Technol. Res. J., 16(5), 147–154, 2022, doi: 10.12913/22998624/153942.
29. M. Pashechko, O. Kharchenk, V. Shcheptov, K. Lenik, and Y. Gladkiy, Features of Formation Stress State of Amorphized Detonation Coatings of the Zr-Al-B Systems. Adv. Sci. Technol. Res. J., 13(2), 46–50, 2019, doi: 10.12913/22998624/106161.
30. A.G. Shtukenberg, M. D. Ward, and B. Kahr, Crystal growth inhibition by impurity stoppers, now. J. Cryst. Growth, 597, 126839, 2022, doi: 10.1016/j.jcrysgro.2022.126839.
31. R. Tran et al., Surface energies of elemental crystals. Sci. Data, 3(1), 160080, 2016, doi: 10.1038/sdata.2016.80.
32. J.J. Gilman, Direct Measurements of the Surface Energies of Crystals. J. Appl. Phys., 31(12), 2208–2218, Dec. 1960, doi: 10.1063/1.1735524.
33. Z. Suo, J. Dai, S. Gao, and H. Gao, Effect of transition metals (Sc, Ti, V, Cr and Mn) doping on electronic structure and optical properties of CdS. Results Phys., 17, 103058, 2020, doi: 10.1016/j.rinp.2020.103058.
34. C. Anastasescu et al., Defect-related light absorption, photoluminiscence and photocatalytic activity of SiO2 with tubular morphology. Sol. Energy Mater. Sol. Cells, 59, 325–335, 2017, doi: 10.1016/j.solmat.2016.09.032.
35. A.G. Shenstone, The third spectrum of copper (cu III). J. Res. Natl. Bur. Stand. Sect. A Phys. Chem., 79A(3), 497, 1975, doi: 10.6028/jres.079A.014.
36. D. Luo, A.K. Pradhan, H.E. Saraph, P.J. Storey, and Y.Yu, Atomic data for opacity calculations. X. Oscillator strengths and photoionisation cross sections for O III. J. Phys. B At. Mol. Opt. Phys., 22(3), 389–406, 1989, doi: 10.1088/0953-4075/22/3/006.